Enhancing Intensity Differences in EEG Cross-Frequency Coupling Maps for Dyslexia Detection

Diego Castillo-Barnes[1,2], Andrés Ortiz[1,2], Pietro Stabile[3], Nicolás J. Gallego-Molina[1,2], Patricia Figueiredo[3], and Juan L. Luque[4]

[1] Communications Engineering Department
University of Málaga. 29004 Málaga, Spain
[2] Andalusian Data Science and Computational Intelligence Institute (DaSCI)
[3] Institute for Systems and Robotics (Lisboa / LARSyS) and Department of Bioengineering, Instituto Superior Técnico, Universidade de Lisboa, Av. Rovisco Pais 1, 1049-001, Lisboa, Portugal
[4] Department of Developmental and Educational Psychology, University of Málaga.29004 Málaga, Spain diegoc@uma.es

Abstract. In this study, we introduced and applied a novel histogram transformation technique to enhance the interpretability and discriminative power of Cross-Frequency Coupling (CFC) maps derived from EEG signals for dyslexia detection. Our approach addresses the challenge of subtle intensity differences in CFC maps, which can hinder the accurate identification of dyslexia-related patterns.
Through visual inspection and quantitative analysis, we demonstrated the effectiveness of the histogram transformation technique in amplifying intensity differences within CFC maps. Specifically, our results show significant improvements in the significance of CFC map pixels, particularly in the Alpha-Beta coupling band, post-transformation. This enhancement in discriminative power was further supported by the reduction in entropy and the identification of texture feature changes through Gray-Level Co-occurrence Matrix (GLCM) analysis.

Keywords: EEG · Cross-Frequency Coupling · Dyslexia · Image processing · Histogram transformation · Mann-Whitney-Wilcoxon · Cross-Entropy · GLCM · Interpretability

1 Introduction

Dyslexia, a neurodevelopmental disorder, influences learning abilities such as reading and linguistic skills. The early diagnosis of this disorder allows customized instruction for affected children, improving their academic success and self-esteem [30]. Diagnosing dyslexia often involves assessing a child's reading accuracy, fluency, and understanding. However, traditional diagnosis methods may not capture the full spectrum of dyslexia symptoms due to the disorder's complex and diverse nature [23,25,33].

To address this challenge, novel techniques such as Cross-Frequency Coupling (CFC) from electroencephalogram (EEG) signals are increasingly being used to discern brain activity differences (even if they may be related with cognition or other behavioural aspects) in dyslexic individuals [6,3,29]. These techniques, analyzing either phase-amplitude and phase-phase coupling values, demonstrate effective detection of dyslexia-related networks in the brain, paving the way towards early intervention and improved therapeutic outcomes [17,18,20,21].

While artificial intelligence techniques analyzing EEG bands have been in the spotlight in recent years, yielding significant insights into dyslexia's biological underpinnings, works such as [14,13,16,15,4] present two main challenges: 1) the loss of interpretability, especially when applying techniques like Principal Component Analysis (PCA) and Holo-Hilbert Spectral Analysis (HHSA), and 2) the identification of intricate patterns that are especially crucial in the early stages of this disorder.

In this context, this work steers the spotlight towards the proposal and application of a novel histogram transformation technique to amplify intensity differences in the CFC maps between patients and controls. This unique approach aims to bridge the limitations observed in prior models by accentuating the edges of the regions of interest, thereby enabling easier discerning of controls and dyslexics. For that, our method takes the original CFC maps and transforms the activations of each pixel to their corresponding bin height in the histogram. This technique enhances the activation bounds within the CFC maps, especially in the absence of differentiated isolated activations, making it much easier for potential classifiers to distinguish dyslexic individuals from controls. Note that, done correctly, these new markers could offer deeper insights into dyslexia by accurately determining which brain areas are more related to developmental dyslexia, and revealing any potential associations between different brain regions.

In this work, we unravel our proposed histogram transformation model's strengths, unique features, and potential to drive more accurate early dyslexia detection. We hope that our novel contribution can inspire further research in this direction with a profound ripple effect on the futures of children with dyslexia.

2 Materials & Methods

2.1 Database

For this work we have made use of a dataset provided by the LEEDUCA research group at the University of Malaga (Spain) [24]. This dataset is the result of a comprehensive longitudinal study involving over 1400 children aged 4 to 8 years, all of whom underwent regular assessments involving cognitive and linguistic tasks. In this case, we randomly selected the EEG signals from a subset of 15 children diagnosed with dyslexia and a control group comprising 33 neurotypical children, all matched for age and socio-economic indices.

During the EEG acquisition, each child is exposed to auditory stimuli consisting of amplitude-modulated white noise presented at varying rates: 4.8 Hz, 16 Hz, and 40 Hz to encapsulate the core units of common language speech (Spanish). Each EEG recording session lasts 15 minutes (5 minutes for each frequency), during which the stimuli are presented continually and sequentially in a specific order: $[4.8 \rightarrow 16 \rightarrow 40]$ Hz (ascending) and $[40 \rightarrow 16 \rightarrow 4.8]$ Hz (descending). The EEG data were acquired using a Brainvision actiCHamp Plus system (www.brainproducts.com) with actiCAP electrodes configured to a 32-channel 10-20 layout and optimized specifically for auditory processing. Moreover, the EEG signals have been previously processed to remove artifacts induced by eye blinks, using an Independent Component Analysis (ICA); to normalize individual channels to zero mean and unit variance; to ensure a reference to the Cz electrode; and to undergo baseline correction.

Ethical approval for this study was obtained from the Medical Ethics Committee of the University of Malaga (`CEUMA 16-2020-H`), and written consent was obtained from the tutors in accordance with the Declaration of Helsinki of the World Medical Association. The research has the support of the *Consejería de Educación de la Junta de Andalucía* (Spain), facilitating its implementation in a number of public schools.

2.2 Generation of CFC maps from EEG signals

CFC measures in EEG signals help us to quantify the interactions (coordination) between different frequency bands in the brain. Although the most traditional approach consists of analyzing how the phase of one frequency band influences the amplitude of another frequency band, we have focused on evaluating phase-phase couplings since these kind of interactions play a crucial role in various cognitive processes such as memory, attention, and perception [26,29].

For CFC analysis, we have used a modification of the Intersite Phase Clustering (ISPC) method [9], termed CFS (Cross-Frequency phase Synchronization), focusing on the distribution of phase angle differences between frequency bands within the same electrode. The CFS measure is computed as the absolute mean phase difference between two frequency bands over time intervals, as shown in Equation 1.

$$\mathrm{CFS}_{A,B} = \left| \frac{1}{n} \sum_{t=1}^{n} e^{i(\phi_A(t) - \phi_B(t))} \right| \tag{1}$$

Here, $\phi_A(t)$ and $\phi_B(t)$ represent the phase angles for frequency bands A and B respectively, and n is the number of time points. We focus on Delta ($0.5 - 4$ Hz), Theta ($4 - 8$ Hz), Alpha ($8 - 12$ Hz), Beta ($12 - 30$ Hz), and Gamma ($30 - 80$ Hz) frequency bands. Filtered EEG signals are processed using Hilbert Transform to extract instantaneous phase, facilitating the computation of CFS values [11].

To visualize CFS maps, we project EEG electrode locations onto a 2D reference space using an Azimuthal Equidistant Projection method [5]. Interpo-

lating CFS values between electrodes using Clough-Tocher interpolation [2], we generate maps representing spatial phase-phase coupling distributions between frequency bands. Figure 1 presents CFS maps derived from EEG signals of a randomly selected subject in the dataset, depicting spatial patterns of cross-frequency interactions.

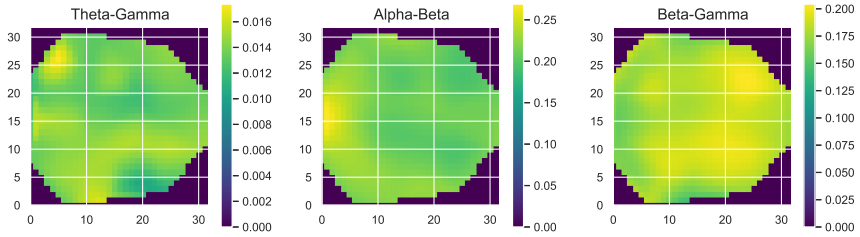

Fig. 1. CFS maps across the scalp illustrating different coupling bands for our EEG analysis. Results obtained by averaging the data from a randomly selected subject in the LEEDUCA platform dataset. Exposure to a white noise auditory stimulus at 4.8 Hz.

2.3 Enhancing differences in CFS maps through histogram transformation

While CFS maps can provide valuable insights, the differences in value are often subtle and challenging for visual interpretation and further image processing steps. In this context, there are many methods from which we could try to enhance the differences in CFS maps, such as Adaptive Histogram Equalization [28,32], Contrast-Stretching [31], Gradient-Based Enhancement [8], Logarithmic-transformation [1], Contrast Enhancement using Discrete Wavelet Transform [10], Local Laplacian Filters [27], among others. However, when we analyze the CFS intensity maps in Figure 1 and their associated histograms in Figure 2, we realize that these histograms showcase narrow distributions because the intensity differences of the original images are relatively minor. This characteristic makes it challenging for any classifier to distinguish between controls and dyslexics based solely on these intensity values.

To mitigate this, we propose applying a simple but effective histogram transformation on the CFS maps. This technique consists of replacing the activations or intensity values of each pixel in CFS maps with the corresponding height of the bin in the histogram obtained from the map's original intensities. Since this height becomes our new intensity value, it intensifies the variation between different values, leading to enhanced differences and better visual separation of the

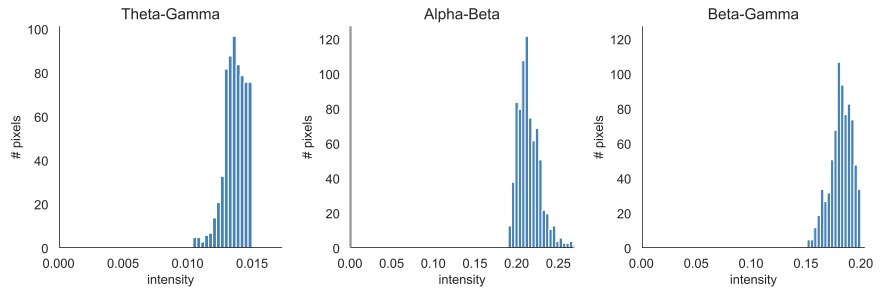

Fig. 2. Histograms illustrating the distribution of CFS intensity values for different coupling bands in the EEG analysis. Each histogram corresponds to a specific frequency band: Theta-Gamma, Alpha-Beta and Beta-Gamma.

features of interest in the histogram-equalized CFS maps whose subtle intensity differences might be clinically significant.

Mathematically, this transformation can be described as follows:

- Let I_{orig} denote the original CFS map, then its histogram can be obtained as $H_{orig} = hist(I_{orig}, N_b)$, where $hist(.,.)$ is the histogram function and N_b is the number of bins.
- Let $h(i)$ be the height of bin i, where $i \in 1, ..., N_b$, then the histogram transformed CFS map, I_{trans} can be obtained as $I_{trans} = h(I_{orig})$ where $h(.)$ is the function that maps each intensity value in I_{orig} to its corresponding bin height in the histogram.

Following the application of this transformation to the CFS intensity maps depicted in Figure 2, the resulting spatial distributions of intensity values, as illustrated in Figure 3, reflect an accentuation of differences between regions, facilitated by the mapping of each intensity value to its corresponding bin height in the histogram.

2.4 Quantification of the improvement

To quantify the enhancement achieved by the histogram transformation of the CFS maps, we employ two distinct metrics: the Mann-Whitney-Wilcoxon U-Test and Cross-Entropy analysis. Additionally, we assess changes in GLCM (Gray-Level Co-occurrence Matrix) properties pre- and post-transformation to understand texture feature alterations.

Mann-Whitney-Wilcoxon U-Test The Mann-Whitney-Wilcoxon U-Test is a non-parametric statistical test used to determine whether there is a significant difference between two independent groups [12]. In our study, we utilize this test to compare the distributions of CFS map pixel values before and after

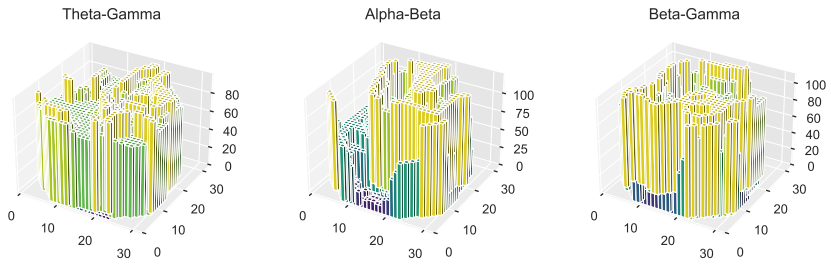

Fig. 3. Transformation of CFS intensity maps using histogram enhancement. Each subplot represents the spatial distribution of intensity values after applying the enhancement method to the CFS maps corresponding to different frequency coupling bands. The color of each voxel represents the height of the histogram bin associated with its intensity value, accentuating differences between regions.

histogram transformation for different band couplings. The null hypothesis is that the distributions of the two groups are equal, and a low $p-$value indicates a rejection of this hypothesis, suggesting a significant difference between the distributions.

Cross-Entropy Cross-Entropy is a measure commonly used to assess the difference between two probability distributions. In our context, it allows us to quantify the change in entropy of coupling band distributions before and after histogram transformation. A decrease in cross-entropy indicates a reduction in uncertainty or disorder within the coupling, while an increase signifies greater uncertainty or disorder. The formula for cross-entropy is given by (2), where $p(i)$ and $q(i)$ represent the probability distributions before and after transformation, respectively.

$$H(p,q) = -\sum_{i} p(i)\log(q(i)) \tag{2}$$

Grey-Level Co-occurrence Matrix (GLCM) GLCM analysis provides insights into texture feature changes pre- and post-transformation by assessing pixel relationships within the CFS maps. We compute GLCM properties such as Contrast, Dissimilarity, Homogeneity, Energy, and Correlation for each coupling band. These properties quantify the spatial relationships between pixel values and enable the characterization of texture features within the maps [22].

3 Results

Visual inspection of the average CFS maps, derived from the 33 controls (top row) and 15 dyslexics children (bottom row) from the LEEDUCA subset, both

before and after histogram transformation, reveals discernible differences in the intensity activations of CFS maps (Figure 4 for Alpha-Beta coupling, Figure 5 for Beta-Gamma coupling, and Figure 6 for Theta-Gamma coupling).

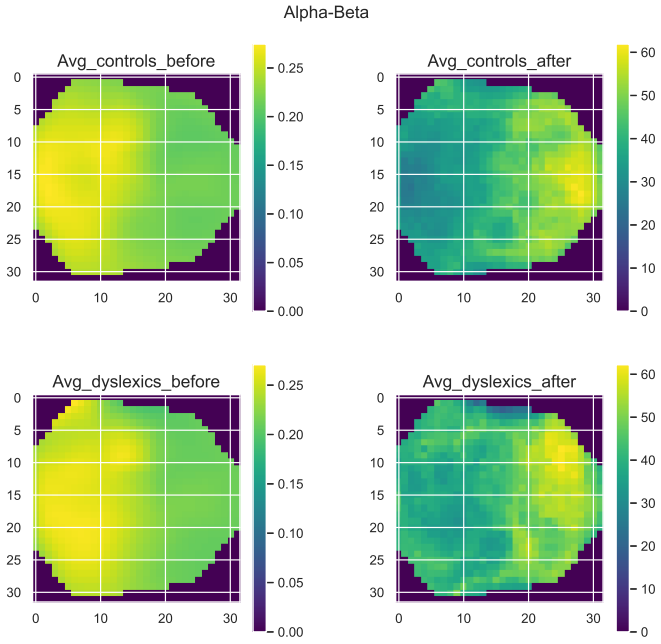

Fig. 4. Comparison of averaged CFS maps derived from control subjects and those with dyslexia for Alpha-Beta couplings before (left column) and after (right column) histogram transformation.

Analysis of the negative logarithm of the p_{values}, arranged in descending order (Figure 7), indicates a pronounced increase in the significance of CFS map pixels in the alpha-beta band following histogram transformation. While some improvements are observed in other bands post-transformation, the differences between pre- and post-transformation curves are less prominent.

Cross-entropy analysis offers insights into the transformation's impact on coupling band entropy. For Theta-Gamma coupling, the initial cross-entropy of -1269.67 increased to -1419.57 post-transformation, indicating reduced entropy. Similarly, Alpha-Beta coupling exhibited a substantial increase in cross-entropy from -408.25 to -1338.35, suggesting decreased entropy. Surprisingly, Beta-Gamma coupling displayed a dramatic rise in entropy from -525.45 to 2165.82 after transformation, signifying increased disorder within the coupling.

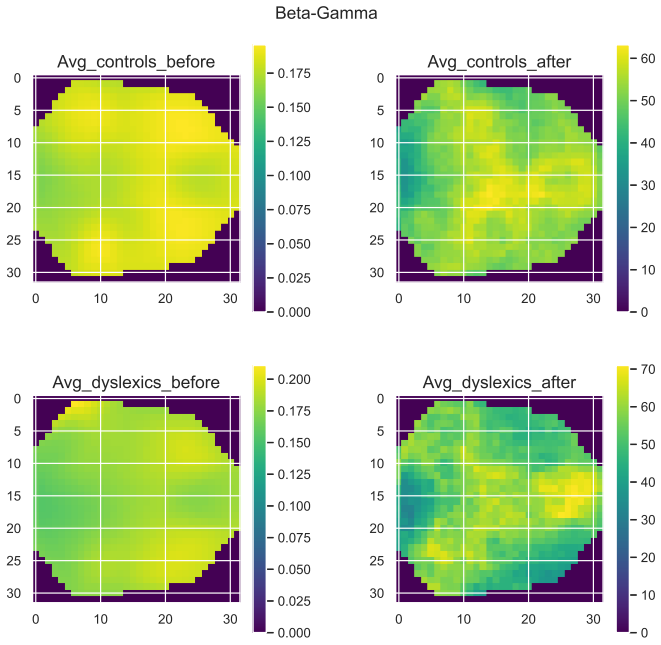

Fig. 5. Comparison of averaged CFS maps derived from control subjects and those with dyslexia for Beta-Gamma couplings before (left column) and after (right column) histogram transformation.

Furthermore, GLCM properties were assessed to discern texture feature changes pre- and post-transformation. Before transformation, T-tests showed no significant differences in GLCM properties. However, post-transformation:

Theta-Gamma Coupling:

- Contrast remained largely unchanged ($p_{\text{value}} = 0.1795$).
- Dissimilarity exhibited a significant decrease ($p_{\text{value}} = 0.0284$), indicating reduced heterogeneity.
- Homogeneity notably increased ($p_{\text{value}} = 0.0008$), suggesting greater uniformity in pixel value distributions.
- Energy showed no significant alteration ($p_{\text{value}} = 0.1688$).
- Correlation remained unchanged ($p_{\text{value}} = 0.8859$).

Alpha-Beta Coupling:

- Contrast remained stable ($p_{\text{value}} = 0.8033$).
- Dissimilarity showed no substantial change ($p_{\text{value}} = 0.5292$).
- Homogeneity remained unchanged ($p_{\text{value}} = 0.2425$).
- Energy exhibited no significant difference ($p_{\text{value}} = 0.9627$).
- Correlation showed no significant change ($p_{\text{value}} = 0.9637$).

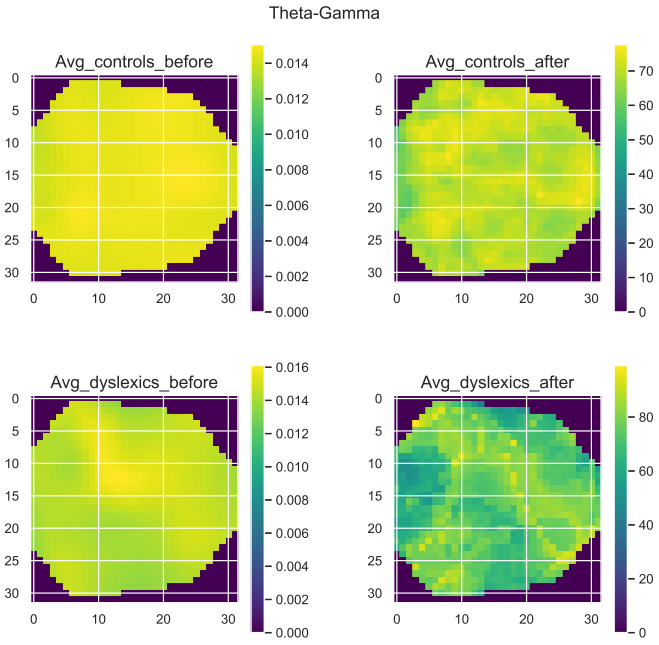

Fig. 6. Comparison of averaged CFS maps derived from control subjects and those with dyslexia for Theta-Gamma couplings before (left column) and after (right column) histogram transformation.

Beta-Gamma Coupling:

- Contrast remained unchanged ($p_{\text{value}} = 0.6824$).
- Dissimilarity showed no substantial alteration ($p_{\text{value}} = 0.2325$).
- Homogeneity significantly increased ($p_{\text{value}} = 0.0119$), indicating greater uniformity.
- Energy remained unaffected ($p_{\text{value}} = 0.4984$).
- Correlation showed no significant change ($p_{\text{value}} = 0.7648$).

4 Discussion & Conclusions

EEG-based techniques have emerged as pivotal tools in unraveling the neurobiological underpinnings of dyslexia, as evidenced by studies conducted by Gallego Molina et al. [14,16] or Attaheri et al. [4] among others. In this context, our histogram transformation technique applied to the CFS maps presents a promising avenue for enhancing the detection of dyslexia as its application to narrow histograms or 'low-contrast' CFS maps can help to accentuate the differentiation between the pixels' intensity levels and raise classifiers' performance even under

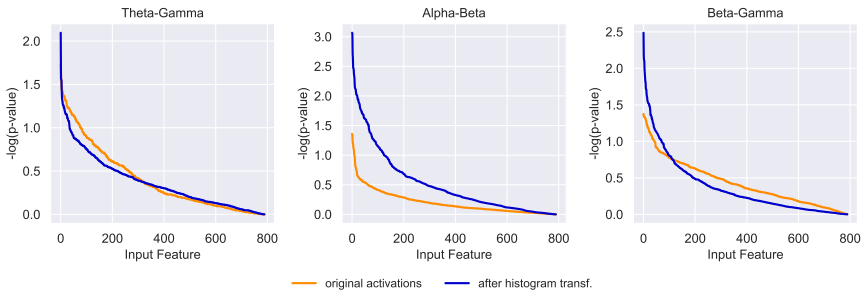

Fig. 7. Negative logarithm of p-values from Mann-Whitney-Wilcoxon U-Test for different band couplings before and after histogram transformation. The term 'Input Feature' denotes the pixels of the unraveled CFS maps, arranged in descending order based on their corresponding $-log(p_{\text{value}})$ values.

these challenging conditions. While other existing techniques, such as [19,7,1], focus on histogram modifications for image enhancement and normalization in various domains, our approach stands out for its specific application to the enhancement of images whose activation patterns are very subtle and homogeneous. In contexts where there are not a few isolated pixels whose sparse activations are what really make a classifier good at distinguishing between classes (as it happens with the CFC couplings where a cluster of neurons influences on the behaviour of another group of a different level), this means that we are able to enhance this effect and visualize it more clearly, helping us not only to improve the interpretability of our CFS maps but also identifying better which neuronal regions are more related to dyslexia.

Starting with the visual inspection of the average CFS maps before and after histogram transformation in Figures 4, 5, and 6, our findings reveal discernible differences in intensity activations, particularly pronounced in the Alpha-Beta coupling. These differences, quantified using statistical methods, demonstrate a significant increase in the significance of CFS map pixels post-transformation, as indicated by the Mann-Whitney-Wilcoxon U-Test results (see Figure 7). Notably, this Alpha-Beta coupling band exhibits a remarkable improvement in significance post-transformation, suggesting that the histogram transformation effectively enhances the discriminative power of the CFS maps.

The observed reduction in entropy for Theta-Gamma and Alpha-Beta couplings, as highlighted by the Cross-Entropy analysis, further supports the effectiveness of the proposed method in reducing uncertainty or disorder within these couplings. This reduction implies a clearer delineation of patterns within the CFS maps, which can facilitate more accurate classification between control subjects and those with dyslexia. Moreover, the texture feature changes identified through GLCM analysis provide additional insights into the transformation's impact on the spatial distribution of pixel values within the CFS maps. These changes, including decreases in dissimilarity and increases in homogeneity,

underscore the transformation's role in promoting a more uniform distribution of intensity values, thereby enhancing the discriminative features of CFS maps.

In summary, our novel histogram transformation technique represents a significant advancement in dyslexia research using EEG-based analysis. By addressing the challenge of subtle intensity differences in CFC maps, our approach offers several key advantages. Firstly, it enhances the interpretability of CFC maps by facilitating clearer delineation of patterns, thereby aiding in the identification of dyslexia-related networks in the brain. This improvement in interpretability is crucial for gaining deeper insights into the neurobiological mechanisms underlying dyslexia. Secondly, our technique significantly boosts the discriminative power of CFC maps, potentially enhancing the accuracy of dyslexia detection algorithms. By improving the ability to differentiate between dyslexic individuals and controls, our method contributes to more reliable diagnostic outcomes, which is essential for effective intervention strategies. Lastly, our approach is computationally efficient and seamlessly integrates into existing CFC analysis pipelines, making it practical for real-time dyslexia detection systems. Its feasibility for deployment in clinical settings underscores its potential to impact dyslexia diagnosis and intervention on a broader scale.

Acknowledgments

This research is part of the PID2022-137461NB-C32, PID2022-137629OA-I00 and PID2022-137451OB-I00 projects, funded by the MCIN/ AEI/ 10.13039/ 501100011033 and by FSE+ as well as UMA20-FEDERJA-086 (Consejería de econnomía y conocimiento, Junta de Andalucía) and by European Regional Development Funds (ERDF) and NextGenerationEU. Work by D.C.B. is supported by the MCIN/AEI/FJC2021-048082-I 'Juan de la Cierva Formacion'. Marco A. Formoso grant PRE2019-087350 funded by MCIN/AEI/ 10.13039/501100011033 by "ESF Investing in your future". LARSyS funding (DOI: 10.54499/LA/P/0083/2020, 10.54499/UIDP/50009/2020, and the 10.54499/UIDB/50009/2020).

References

1. Agaian, S.S., Silver, B., Panetta, K.A.: Transform coefficient histogram-based image enhancement algorithms using contrast entropy. IEEE Transactions on Image Processing **16**(3), 741–758 (Mar 2007). https://doi.org/10.1109/tip.2006.888338
2. Alfeld, P.: A trivariate clough—tocher scheme for tetrahedral data. Computer Aided Geometric Design **1**(2), 169–181 (Nov 1984). https://doi.org/10.1016/0167-8396(84)90029-3
3. Aru, J., Aru, J., Priesemann, V., Wibral, M., Lana, L., Pipa, G., Singer, W., Vicente, R.: Untangling cross-frequency coupling in neuroscience. Current Opinion in Neurobiology **31**, 51–61 (apr 2015). https://doi.org/10.1016/j.conb.2014.08.002
4. Attaheri, A., Choisdealbha, Á.N., Rocha, S., Brusini, P., Di Liberto, G.M., Mead, N., Olawole-Scott, H., Boutris, P., Gibbon, S., Williams, I., Grey, C., e Oliveira, M.A., Brough, C., Flanagan, S., Goswami, U.: Infant low-frequency eeg cortical power, cortical tracking and phase-amplitude coupling predicts language a year later (Nov 2022). https://doi.org/10.1101/2022.11.02.514963

5. Bashivan, P., Rish, I., Yeasin, M., Codella, N.: Learning representations from eeg with deep recurrent-convolutional neural networks (2015). https://doi.org/10.48550/ARXIV.1511.06448
6. Canolty, R.T., Knight, R.T.: The functional role of cross-frequency coupling. Trends in Cognitive Sciences **14**(11), 506–515 (nov 2010). https://doi.org/10.1016/j.tics.2010.09.001
7. Chang, D.C., Wu, W.R.: Image contrast enhancement based on a histogram transformation of local standard deviation. IEEE Transactions on Medical Imaging **17**(4), 518–531 (1998). https://doi.org/10.1109/42.730397
8. Chaple, G.N., Daruwala, R.D., Gofane, M.S.: Comparisions of robert, prewitt, sobel operator based edge detection methods for real time uses on fpga. In: 2015 International Conference on Technologies for Sustainable Development (ICTSD). IEEE (Feb 2015). https://doi.org/10.1109/ictsd.2015.7095920
9. Cohen, M.: Analyzing Neural Time Series Data: Theory and Practice (01 2014). https://doi.org/10.7551/mitpress/9609.001.0001
10. Demirel, H., Ozcinar, C., Anbarjafari, G.: Satellite image contrast enhancement using discrete wavelet transform and singular value decomposition. IEEE Geoscience and Remote Sensing Letters **7**(2), 333–337 (Apr 2010). https://doi.org/10.1109/lgrs.2009.2034873
11. Dvorak, D., Fenton, A.A.: Toward a proper estimation of phase-amplitude coupling in neural oscillations. Journal of Neuroscience Methods **225**, 42–56 (mar 2014). https://doi.org/10.1016/j.jneumeth.2014.01.002
12. Fay, M.P., Proschan, M.A.: Wilcoxon-mann-whitney or t-test? on assumptions for hypothesis tests and multiple interpretations of decision rules. Statistics Surveys **4** (jan 2010). https://doi.org/10.1214/09-ss051
13. Formoso, M.A., Ortiz, A., Martinez-Murcia, F.J., Gallego, N., Luque, J.L.: Detecting phase-synchrony connectivity anomalies in EEG signals. application to dyslexia diagnosis. Sensors **21**(21), 7061 (oct 2021). https://doi.org/10.3390/s21217061
14. Gallego-Molina, N.J., Formoso, M., Ortiz, A., Martínez-Murcia, F.J., Luque, J.L.: Temporal EigenPAC for dyslexia diagnosis. In: Advances in Computational Intelligence, pp. 45–56. Springer International Publishing (2021). https://doi.org/10.1007/978-3-030-85099-9_4
15. Gallego-Molina, N.J., Ortiz, A., Martínez-Murcia, F.J., Formoso, M.A., Giménez, A.: Complex network modeling of EEG band coupling in dyslexia: An exploratory analysis of auditory processing and diagnosis. Knowledge-Based Systems **240**, 108098 (mar 2022). https://doi.org/10.1016/j.knosys.2021.108098
16. Gallego-Molina, N.J., Ortiz, A., Martínez-Murcia, F.J., Rodríguez-Rodríguez, I.: Unraveling dyslexia-related connectivity patterns in EEG signals by holo-hilbert spectral analysis. In: Artificial Intelligence in Neuroscience: Affective Analysis and Health Applications, pp. 43–52. Springer International Publishing (2022). https://doi.org/10.1007/978-3-031-06242-1_5
17. Giraud, A.L., Poeppel, D.: Cortical oscillations and speech processing: emerging computational principles and operations. Nature Neuroscience **15**(4), 511–517 (mar 2012). https://doi.org/10.1038/nn.3063
18. Gross, J., Hoogenboom, N., Thut, G., Schyns, P., Panzeri, S., Belin, P., Garrod, S.: Speech rhythms and multiplexed oscillatory sensory coding in the human brain. PLoS Biology **11**(12), e1001752 (dec 2013). https://doi.org/10.1371/journal.pbio.1001752
19. Kautsky, J., Nichols, N.K., Jupp, D.L.: Smoothed histogram modification for image processing. Computer Vision, Graphics, and Image Processing **26**(3), 271–291 (Jun 1984). https://doi.org/10.1016/0734-189x(84)90213-5

20. Keitel, A., Gross, J., Kayser, C.: Perceptually relevant speech tracking in auditory and motor cortex reflects distinct linguistic features. PLOS Biology **16**(3), e2004473 (mar 2018). https://doi.org/10.1371/journal.pbio.2004473
21. Keshavarzi, M., Mandke, K., Macfarlane, A., Parvez, L., Gabrielczyk, F., Wilson, A., Goswami, U.: Atypical beta-band effects in children with dyslexia in response to rhythmic audio-visual speech (mar 2023). https://doi.org/10.1101/2023.03.29.534542
22. Mall, P.K., Singh, P.K., Yadav, D.: Glcm based feature extraction and medical x-ray image classification using machine learning techniques. In: 2019 IEEE Conference on Information and Communication Technology. IEEE (Dec 2019). https://doi.org/10.1109/cict48419.2019.9066263
23. McArthur, G., Kohnen, S., Larsen, L., Jones, K., Anandakumar, T., Banales, E., Castles, A.: Getting to grips with the heterogeneity of developmental dyslexia. Cognitive Neuropsychology **30**(1), 1–24 (feb 2013). https://doi.org/10.1080/02643294.2013.784192
24. Ortiz, A., Martinez-Murcia, F.J., Luque, J.L., Giménez, A., Morales-Ortega, R., Ortega, J.: Dyslexia diagnosis by EEG temporal and spectral descriptors: An anomaly detection approach. International Journal of Neural Systems **30**(07), 2050029 (jun 2020). https://doi.org/10.1142/s012906572050029x
25. Pacheco, A., Reis, A., Araújo, S., Inácio, F., Petersson, K.M., Faísca, L.: Dyslexia heterogeneity: cognitive profiling of portuguese children with dyslexia. Reading and Writing **27**(9), 1529–1545 (feb 2014). https://doi.org/10.1007/s11145-014-9504-5
26. Palva, J.M., Palva, S., Kaila, K.: Phase synchrony among neuronal oscillations in the human cortex. The Journal of Neuroscience **25**(15), 3962–3972 (apr 2005). https://doi.org/10.1523/jneurosci.4250-04.2005
27. Paris, S., Hasinoff, S.W., Kautz, J.: Local laplacian filters: edge-aware image processing with a laplacian pyramid. Communications of the ACM **58**(3), 81–91 (Feb 2015). https://doi.org/10.1145/2723694
28. Pizer, S.M., Amburn, E.P., Austin, J.D., Cromartie, R., Geselowitz, A., Greer, T., ter Haar Romeny, B., Zimmerman, J.B., Zuiderveld, K.: Adaptive histogram equalization and its variations. Computer Vision, Graphics, and Image Processing **39**(3), 355–368 (Sep 1987). https://doi.org/10.1016/s0734-189x(87)80186-x
29. Scheffer-Teixeira, R., Tort, A.B.: On cross-frequency phase-phase coupling between theta and gamma oscillations in the hippocampus. eLife **5** (dec 2016). https://doi.org/10.7554/elife.20515
30. Snowling, M.J., Hulme, C., Nation, K.: Defining and understanding dyslexia: past, present and future. Oxford Review of Education **46**(4), 501–513 (Jul 2020). https://doi.org/10.1080/03054985.2020.1765756
31. Yang, C.C.: Image enhancement by modified contrast-stretching manipulation. Optics & Laser Technology **38**(3), 196–201 (Apr 2006). https://doi.org/10.1016/j.optlastec.2004.11.009
32. Zhu, Y., Huang, C.: An adaptive histogram equalization algorithm on the image gray level mapping. Physics Procedia **25**, 601–608 (2012). https://doi.org/10.1016/j.phpro.2012.03.132
33. Zoubrinetzky, R., Bielle, F., Valdois, S.: New insights on developmental dyslexia subtypes: Heterogeneity of mixed reading profiles. PLoS ONE **9**(6), e99337 (jun 2014). https://doi.org/10.1371/journal.pone.0099337